

## Resource Recovery from Maize Wastes; Synthesis and Characterization of Silicon Oxide Nanoparticles

Fabian James Umoren\* and Mfon Clement Utin

Received: 02 February 2024/Accepted: 30 June 2024/Published: 05 July 2024

**Abstract:** This study presents a preliminary evaluation of maize comb waste as a precursor for the synthesis of bio-silicon oxide nanoparticles (SiONPs). Nanotechnology has emerged as a promising field for various applications, and SiO<sub>2</sub> nanoparticles have garnered significant interest due to their unique properties. However, conventional synthesis methods often involve high energy consumption and the use of toxic chemicals, raising environmental concerns. In this context, exploring eco-friendly precursors is essential for sustainable nanoparticle synthesis. Maize comb waste, a readily available agricultural byproduct rich in silica, was investigated as a potential precursor for SiONP synthesis. The study aimed to assess the feasibility of utilizing this waste material to produce SiONPs in a sustainable and environmentally friendly manner. The synthesized SiONPs exhibited a wavelength of maximum absorption at 310 nm, indicating SiONPs in the ultraviolet range. X-ray diffraction (XRD) analysis confirmed the crystalline nature of the nanoparticles, with an average crystallite size of 12.75 nm. The lattice microstrain ranged from 0.0018 to 0.0048, indicating slight variations across different crystallographic planes. Porosity analysis revealed an average porosity of 0.71%, indicating microporous characteristics suitable for various applications. Remarkably, the packing density of the synthesized SiONPs was found to be 1, suggesting a densely packed structure with minimal void space between nanoparticles. The Brunauer-Emmett-Teller (BET) analysis showed a surface area of 108.395 m<sup>2</sup>/g, pore volume of 569.30 m<sup>3</sup>, and pore size of 2.88 nm. The nanoparticle

diameter calculated from BET parameters was 13.62 nm, indicating microporous characteristics. The results demonstrate the potential of maize comb waste as a sustainable precursor for SiONP synthesis, offering insights into green nanotechnology practices and the utilization of renewable resources for nanomaterial synthesis.

**Keywords:** Resource recovery, biodegradable waste, maize comb, silicon oxide nanoparticles, synthesis and characterization

**Fabian James Umoren\***

Department of Chemistry, Federal Polytechnic, Ukana, Essien Udim Local Government Area, Akwa Ibom State, Nigeria

**Email:** [umorenfabian@yahoo.com](mailto:umorenfabian@yahoo.com)

**Mfon Clement Utin**

Department of Pure and Applied Chemistry, University of Port Harcourt, Port Harcourt, Rivers State, Nigeria,

**Email:** [faustyluv@gmail.com](mailto:faustyluv@gmail.com)

**Orcid id:** [0009-0003-5254-3357](https://orcid.org/0009-0003-5254-3357)

### 1.0 Introduction

Nanotechnology has revolutionized various fields by offering innovative solutions and enhancing the performance of materials through the manipulation of matter at the nanoscale (Eddy *et al.*, 2024a-b). Among the diverse range of nanomaterials, silicon oxide (SiO<sub>2</sub>) nanoparticles have gained significant attention due to their unique properties, such as high surface area, chemical stability, and biocompatibility (Eddy *et al.*, 2023a-c; Garg *et al.*, 2022).. These attributes make SiO<sub>2</sub> nanoparticles ideal for applications in electronics, biomedicine, environmental remediation, and catalysis (Murugan *et al.*,

2020; Zhang et al., 2021). However, the conventional methods of producing SiO<sub>2</sub> nanoparticles often involve high energy consumption, the use of expensive raw materials, poor management of operation conditions and the use of toxic chemicals, raising concerns about their environmental impact and sustainability (Kumar et al., 2019; Garg et al., 2024).

In response to these challenges, there has been a growing interest in exploring eco-friendly and cost-effective alternatives for the synthesis of SiO<sub>2</sub> nanoparticles. Agricultural waste, a readily available and renewable resource is one of the promising precursors for producing various nanomaterials including silicon oxide nanoparticles. Maize comb waste, in particular, presents a potential candidate due to its high silica content and abundance as a byproduct of maize cultivation (Singh et al., 2022). Consequently, the current study aims to conduct a preliminary evaluation of the suitability of maize comb waste as a precursor for bio-silicon oxide nanoparticles, focusing on its potential to provide a sustainable and environmentally friendly source of SiO<sub>2</sub>.

The global demand for nanomaterials, including SiO<sub>2</sub> nanoparticles, is rapidly increasing, driven by advancements in technology and the need for high-performance materials. Traditional synthesis methods for SiO<sub>2</sub> nanoparticles, such as sol-gel processes and chemical vapour deposition, are effective but often associated with significant environmental and economic costs (Kao et al., 2014). These methods typically require substantial energy inputs and involve hazardous chemicals, which pose risks to both human health and the environment.

In recent years, the utilization of agricultural waste as a raw material for nanomaterial production has gained momentum. This approach not only addresses the issue of waste management but also offers a sustainable pathway for producing high-value materials. Various studies have demonstrated the

feasibility of using agricultural residues, such as rice husks, wheat straw, and sugarcane bagasse, for synthesizing SiO<sub>2</sub> nanoparticles (Ahmad et al., 2018; Li et al., 2021). Maize comb waste, an underutilized byproduct of maize harvesting, contains significant amounts of silica, making it a potential resource for SiO<sub>2</sub> nanoparticle synthesis.

Maize (*Zea mays* L.) is one of the most widely cultivated crops globally, with millions of tons of maize comb waste generated annually. Despite its high silica content, this biomass is often discarded or used for low-value applications, such as animal feed or fuel (Dube et al., 2022). The valorization of maize comb waste for producing SiO<sub>2</sub> nanoparticles not only offers a sustainable solution for waste management but also contributes to the circular economy by converting agricultural residues into valuable nanomaterials.

This study aims to evaluate the feasibility of using maize comb waste as a precursor for SiO<sub>2</sub> nanoparticles. By exploring the physicochemical properties of the derived nanoparticles and assessing their potential applications, this research seeks to provide insights into the viability of this sustainable approach. The findings are expected to contribute to the development of green nanotechnology practices and promote the use of renewable resources in nanomaterial synthesis.

## 2.0 Materials and Methods

The precursor was collected freely from some farmlands within the University of Nigeria, Nsukka. Reagents used for the study were, 2 M analytical grade HCl, NaOH pellets and distilled water. The silicon nanoparticles were synthesised using the sol-gel method (Eddy et al., 2024a) and characterized using UV visible, XRD and BET.

## 3.0 Results and Discussion

The UV visible absorption spectrum of silicon oxide nanoparticles (SiONPs) synthesized from maize stalk is shown in Fig. 1. The



spectrum indicates that the wavelength of maximum absorption ( $\lambda_{max}$ ) by the silicon oxide nanoparticles is 310 nm which indicates that the nanoparticles absorb in the ultraviolet range (Ogoko et al., 2023). Based on Planck’s equation, the expected band gap of the SiONPs can be evaluated using equation .1 (Eddy et al., 2023d-f)

$$E_{BG} = \frac{hc}{\lambda_{max}} \quad (1)$$

where h is the Planck constant and c is the speed of light. The insertion of the numerical constants and  $\lambda_{max}$  into equation 1 indicates that the bandgap of the nanoparticles is equal to 4.2 eV. The observed  $\lambda_{max}$  shows some relative levels of agreement with values

reported elsewhere. For example,  $\lambda_{max}$  of 235 nm has been reported for silicon oxide nanoparticles synthesized by the sol-gel method by Hussin, et al. (2016).  $\lambda_{max}$  of 297 nm has also been reported by Biradar et al. (2021) for SiONPs and 485 nm by Intartaglia et al. (2012). The significance of the wavelength of maximum absorption is that it is a measure of the identity of the nanoparticles and based on the comparative values to literature reports, the synthesized materials a SiONPs. The measure bandgap shows that the material is a semiconductor and can be an effective dopant and photocatalyst among other applications

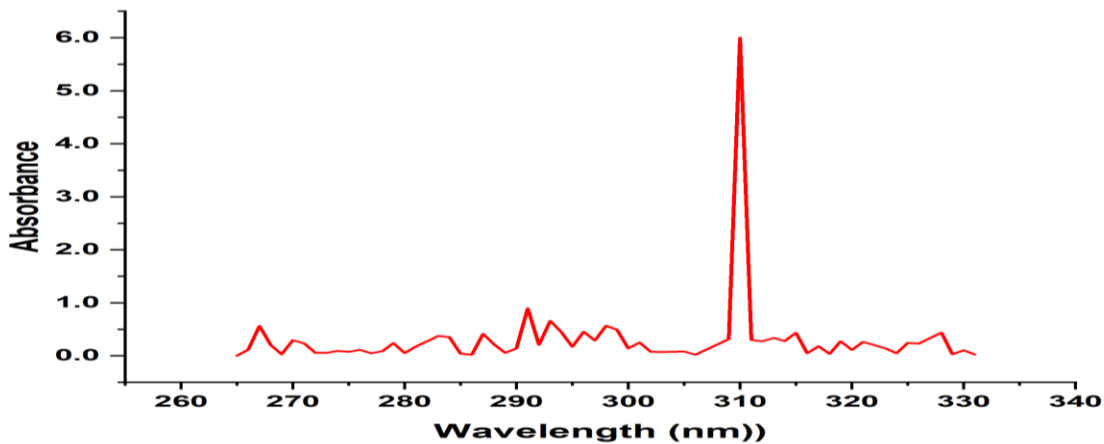


**Fig. 1: UV visible absorption spectrum of SiONPs synthesized from maize stalk**

The X-ray diffraction spectrum of the synthesized SIONPs is shown in Fig. 2 as a plot of intensity against two times the angle of diffraction. From the spectrum, the principal peak was observed at  $46.56^\circ$  while the minor peaks were observed at  $30.48^\circ$ ,  $32.02^\circ$ ,  $35.56^\circ$  and  $38.32^\circ$ . According to Hodhod et al. (2019), a broad XRD peak between  $20^\circ$  and  $30^\circ$  is attributed to amorphous SiONPs while Abdul Ghani et al. (2017) and Rahimzadeh et al. (2022) observed an amorphous peak between  $15^\circ$  and  $35^\circ$  diffraction angle. On the other hand, Daulay et al. (2022) observed absorption peaks at  $28.38^\circ$ ,  $47.26^\circ$ ,  $56.08^\circ$ , and  $69.08^\circ$ . The peaks reflected those expected for crystalline SiONPs. Therefore, a crystalline nature seems to dominate the spectrum. Less noise was

observed, which is unique for the XRD of amorphous crystals (Odoemelam et al., 2023). The spectrum obtained in the study shows a unique match to that of crystalline SIONPs on a reference model of on JCPDS Card No. 00–026–1481.

The determination of crystallite size for the nanoparticles was achieved through the application of Scherrer’s equation (equation .1) which is based on the fact that peak broadening is proportional to the crystallite size (Eddy et al., 2023f-g).

$$D_{Cryst} (nm) = \frac{k\lambda}{L\cos\theta} \quad (2)$$

where  $\theta$  is the angle of diffraction, k is the Scherrer’s constant, (0.9)  $\lambda$  is the wavelength of the Cu-K X-ray ( $\lambda = 1.5406 \text{ nm}$ ) and L is the full width at half maxima.



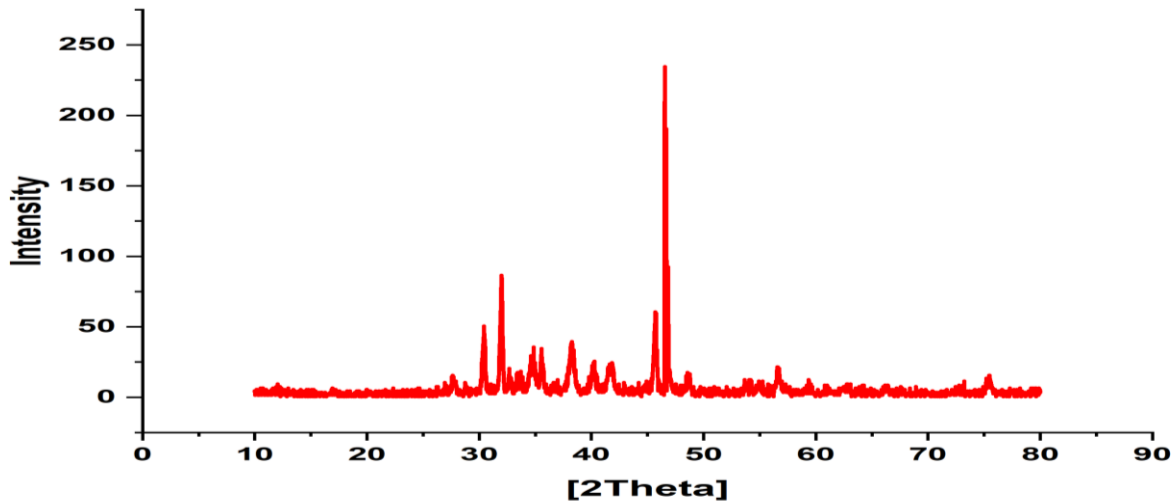


**Fig. 2: XRD spectrum of SiONPs synthesized from maize stalk**

Average crystal parameters were evaluated using origin statistical software, which included  $L = 0.7096$  nm and  $2\theta = 29.36^\circ$ , that is average crystalline size = 12.75 nm, and suggest that the macrostrain, which is the reciprocal of the crystallite size is  $0.0784 \text{ nm}^{-1}$ . The observed value of crystallite size (Tabl 1)

compares favourably with the value of 20 nm reported by Abdul Ghani et al. (2017). Crystallite size as large as 79 nm has been reported by Azib et al., (2021) and could have been probably due to agglomeration. Therefore, the synthesized SiONPs are crystalline and have relatively low crystalline size.

**Table 1: Diffraction parameters for silicon oxide nanoparticles**

$2\theta$	Area	FWHM	$D_{cryst}$ (nm)	$\epsilon$	Miller indices	Phase
29.96	15.68	0.2925	28.11	0.004768	(111)	Cubic phase
31.67	24.52	0.2436	33.89	0.003748	(110)	Alpha cubic or beta cubic phase
45.24	19.41	0.2952	29.15	0.003094	(102)	Monoclinic phase
46.40	27.20	0.1770	48.83	0.001805	(211)	Cubic phase

The miller indices of the nanoparticles were obtained by calculations and by comparing the diffraction pattern with standards. The results indicated results shown in Table 1 above. Based on the provided Miller indices, all four peaks correspond to different phases of silicon oxide:. The diffraction at  $2\theta = 29.96^\circ$  corresponds to the (111) Miller plane and indicates the presence of a cubic phase of silicon oxide, likely alpha-quartz or beta-cristobalite. This peak is described by the Joint Committee on Powder X-ray diffraction

standard (JCDPS) card number equal to 39-1425. At the Miller plane equal to (110), the observed peak suggests a different cubic phase, possibly alpha-quartz or beta-cristobalite (JCPDS= 39-1425) and was observed at  $2\theta = 31.67^\circ$ . At  $2\theta = 45.24^\circ$ , the corresponding plane describing the monoclinic phase of the silicon oxide nanoparticles is (102) with crystallite size equal to 29.15 nm while the JCPDS matching card number is 29.0085. A cubic phase was also observed at  $2\theta = 29.96^\circ$  showing a crystallite size of 48.83 nm and



matching JCPDS card number = 39-1425. The presence of minor peaks however shows that the sample has some impurities, which could be due to the presence of negligible concentrations such as calcium and magnesium in the maize comb sample.

The lattice microstrain was calculated using the rearranged form of the Williamson-Hall equation (equation 2)(Kelle *et al.*, 2023).

$$\varepsilon = \frac{FWHM}{4\tan\theta} + \frac{k\lambda}{D_{cryst}} \quad (3)$$

Microstrain indicates the presence of internal stresses and lattice distortions, which may be from sources, such as dislocations, grain boundaries, vacancies, interstitials, and other crystal defects (Eddy *et al.*, 2023h). Typically, higher microstrain values suggest a greater degree of lattice distortion, which typically indicates a higher density of defects and internal stresses. The mechanical properties of materials, such as hardness, strength, and ductility can be influenced by the level of microstrain. For example, materials with high microstrain may have increased hardness and strength but reduced ductility. Also, microstrain can affect the electronic, optical, and thermal properties of materials. For instance, strained silicon in semiconductor devices can enhance carrier mobility and improve device performance. Finally, microstrain is often considered alongside crystallite size when analyzing materials. While crystallite size affects peak broadening in X-ray diffraction patterns, microstrain contributes to additional peak broadening. Based on the results obtained for the lattice microstrain of the nanoparticles, which ranged from 0.0018 to 0.0048, there is a slight variation in strain across different crystallographic directions (reflected by the Miller indices) within the nanoparticles. The highest strain (0.004768) is observed in peak 1, suggesting a greater distortion of the lattice in that particular direction. All the values are positive, indicating the presence of tensile strain in the silicon oxide nanoparticles. A tensile strain occurs when the lattice is

stretched compared to its ideal configuration. The microstrain values range from approximately 0.001805 to 0.004768. These values indicate varying degrees of internal stresses and lattice distortions across different crystallographic planes in the silicon oxide nanoparticles.

The Porosity of silicon nanoparticles can be calculated in terms of the ratio of pore volume to the total volume of the crystallite, which can be related to the crystallite size according to the following equation

$$Porosity = \frac{V_{pore}}{V_{cryst}} = 1 - \frac{D_{cryst}^3}{D_{cryst}^3 + \frac{0.6}{\varepsilon}} \quad (4)$$

In the above equation, we defined the  $\varepsilon$  as the lattice micro parameter and  $D_{cryst}$  as the crystallite size of the silicon oxide nanoparticles. The evaluated porosity for peaks 1, 2, 3 and 4 were 0.006256, 0.005996, 0.011723 and 0.004455 respectively. The average porosity of the nanoparticles was calculated as 0.007165 (corresponding to 0.71%). The average porosity of 71% falls within the range of microporous materials indicating that the silicon oxide nanoparticles can be classified as microporous materials. Microporous materials generally have porosity levels ranging from 0.5 to 2%. This level of porosity suggests the presence of small nanopores within the material structure. According to recent studies, microporous materials with similar porosity levels have been widely investigated for various applications such as gas separation, catalysis, and drug delivery due to their high surface area and adsorption capacity (Li *et al.*, 2020; Zhang *et al.*, 2021). These materials are known for their ability to adsorb molecules and ions in their nanopores, making them useful in several fields. The findings align with research by Li *et al.* (2020), who studied microporous silicon oxide nanoparticles synthesized via a similar method and reported porosity levels within the microporous range. Similarly, Zhang *et al.* (2021) investigated the applications of microporous silica nanoparticles and



highlighted their potential in drug delivery systems.

The packing density of the silicon oxide nanoparticles was evaluated as the ratio of the volume of silicon oxide nanoparticles to the total volume of the materials as shown by equation 5 below.

$$Packing\ density = \frac{\rho_{bulk}}{\rho_{theor}} \quad (5)$$

We obtained the packing density equivalent to 1, suggesting that the nanoparticles are closely packed within the materials. A packing density of 1 indicates an ideal, densely packed structure with minimal void space between nanoparticles. This parameter is significant for maximizing material properties such as strength, stability, and efficiency, making it desirable for various advanced applications, especially in areas where maximum material density, uniformity and stability are required such as high-performance ceramics, advanced composites, nanoelectronics and catalysts.

The Brunauer-Emmett-Teller (BET) equation can be written according to equation 6 (Ebadi et al., 2009)

$$\frac{1}{X[(P_0/P)-1]} = \frac{1}{X_m} + \frac{C-1}{X_m C} \left(\frac{P}{P_0}\right) \quad (6)$$

A plot representing a multi-BET model is accepted when an excellent linear fitness is obtained from a plot of values of  $\frac{1}{X[(P_0/P)-1]}$  versus the relative pressure defined as  $\left(\frac{P}{P_0}\right)$ .

Therefore, the slope and intercept should also be equal to  $\frac{C-1}{X_m C}$  and  $\frac{1}{X_m}$  respectively. In this model, X defines the amount of N<sub>2</sub> adsorbed at a pressure, P, X<sub>m</sub> represents the monolayer adsorption capacity, P<sub>0</sub> is the initial pressure, and C is a constant. The multi-BET plot for the synthesized SiONPs is shown in Fig. 3. The results obtained from the BET analysis for the synthesized nanomaterials indicated the following properties, BET surface area, pore volume and pore size of 108.395 m<sup>2</sup>/g, 569.30 m<sup>3</sup> and 2.88 nm respectively.

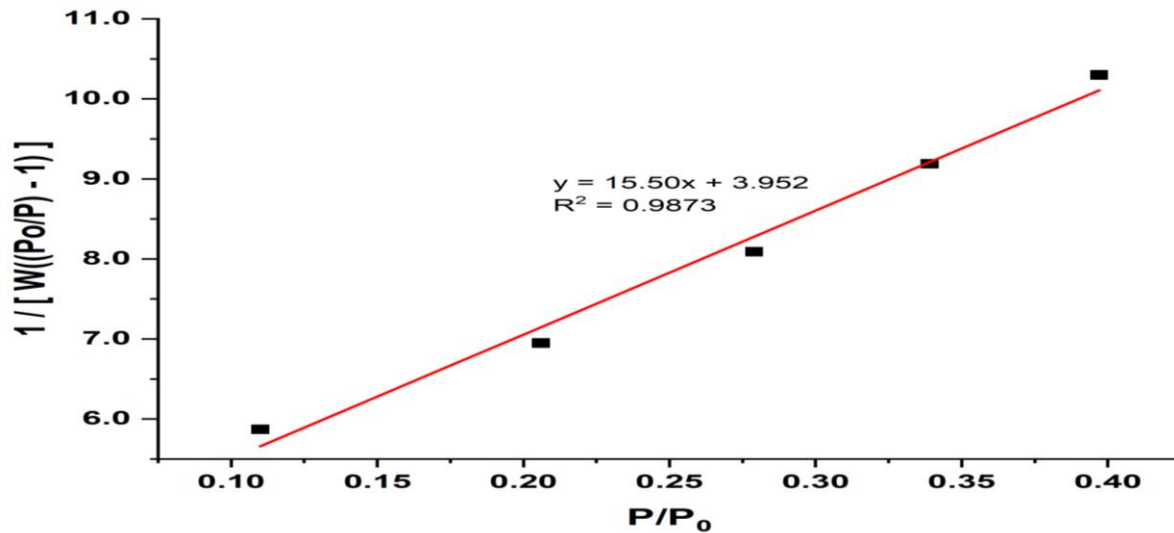


Fig. 3: Multi-BET plot for the synthesized SiONPs

The multiple point BET isotherm for the nitrogen adsorption for the CaONP is shown in Fig. 3. According to Wheeler’s equation, the relationship between nanoparticle diameter, pore volume and surface area can be written as follows (Eddy et al., 2024b),

$$d_{np}(nm) = \frac{4 \times Pore\ volume\ (m^3/g)}{BET\ surface\ area\ (m^2/g)} \quad (7)$$

The substitution of the evaluated parameters into equation 7 gives the diameter of the nanoparticles as 13.62 nm, compared to the BET diameter of 2.08 nm indicating microporous nanoparticles since the particle



size is within the range of 0 to 2 nm nm (Eddy *et al.*, 2024f)

In Table 2, we present some analytical parameters (such as crystallite size and particle

size) for some silicon nanoparticles synthesised from plant wastes and the results show that the present work reveals some improvement compared with previous and recent studies.

**Table 2: Literature values of the properties of silicon oxide nanoparticles from some plant wastes**

Plant Waste Source	Particle Size (nm)	Crystallite Size (nm)	Surface Area (m <sup>2</sup> /g)	Reference
Bamboo Shoots	10-20	5-10	150-200	Lu et al. (2010)
Coffee Grounds	15-25	8-12	100-140	Zhang et al. (2020)
Coconut Fibers	30-40	15-20	70-100	Abdullah et al. (2019)
Coconut Shells	30-50	15-25	80-130	John et al. (2014)
Corn Cobs	20-30	12-15	150-180	Faria et al. (2022)
Corn Stalks	10-20	5-10	200-250	Li et al. (2013)
Cotton Stalks	15-30	8-15	100-150	Li et al. (2014)
Eucalyptus Bark	20-30	12-15	100-130	Fernandes et al. (2014)
Leucaena	10-20	5-10	220-270	Kumar et al. (2019)
Leucocephala Leaves				
Mango Peels	25-35	15-20	110-150	Oladejo et al. (2021)
Napier Grass	30-40	15-20	80-120	Rahman et al. (2012) [
Orange Peels	20-40	10-20	80-120	Zhang et al. (2012)
Orange Pulp	10-20	5-10	180-220	Singh et al. (2018)
Palm Empty Fruit Bunches	40-50	20-25	60-80	Aziz et al. (2017)
Palm Kernel Shells	40-50	20-25	50-80	Aziz & Abdullah (2013)
Peanut Shells	20-30	10-15	120-160	Li et al. (2012)
Pine Needles	15-25	8-12	180-230	Zhu et al. (2008)
Rice Bran	25-35	15-20	130-170	Wang & Song (2014)
Rice Straw Ash	50-70	20-30	40-60	Cui et al. (2011)

**4. Conclusion**

This study explores maize comb waste as a sustainable precursor for bio-silicon oxide nanoparticles (SiONPs) synthesis. The

synthesized SiONPs exhibit promising properties for various applications, indicating the potential of agricultural waste as a valuable resource for nanomaterial synthesis.



Maize comb waste has been successfully utilized to synthesize SiONPs with desirable characteristics, including a crystalline structure, microporous nature, and densely packed arrangement. This approach offers a sustainable solution for nanomaterial synthesis. Based on the findings of the study, we present the following recommendations,

- (i) There is a need for further characterization of the product using other methods (TEM, FTIR, TGA) for comprehensive nanoparticle characterization.
- (ii) We also recommend the optimization of synthesis to enhance SiONPs properties and yield.
- (iii) The investigation of the applications of the SiONPs in biomedicine, catalysis and environmental, industrial and other sectors is recommended.
- (iv) There is a need to evaluate scalability and cost-effectiveness for potential commercialization.

## 5.0 References

- Abdul Ghani, N. A. M., Saeed, M. A. and Hashim, I. H. (2017). Thermoluminescence (TL) response of silica nanoparticles subjected to 50 Gy gamma irradiation. *Malaysian Journal of Fundamental and Applied Sciences*, 13, 3, doi:[10.11113/mjfas.v13n3.593](https://doi.org/10.11113/mjfas.v13n3.593)
- Abdullah, N. H., Aziz, A. A. & Abdullah, H. Z. (2019). Synthesis of silicon nanoparticles from coconut fibers using solution combustion method: Characterization and photocatalytic activity. *Materials Research Express*, 6, 1, 015044. [doi:10.1088/2057-1998/aadf1f]
- Ahmad, T., Bustam, M. A., Mandal, U. K., Ishak, M. R., & Ibrahim, N. A. (2018). Synthesis of silica nanoparticles from rice husks. *Journal of Materials Research and Technology*, 7, 6, pp. 631-636.
- Azib, T., Asehraou, A., Addou, M., Chafik, E. & Salim, M. (2021). Structural and optical characterization of silicon oxide nanoparticles synthesized by sol-gel method. *Optik*, 239, 16659-16687.
- Aziz, A. A., Abdullah, N. H., & Abdullah, H. Z. (2017). Green synthesis of silicon nanoparticles from palm empty fruit bunches using solution combustion method: Characterization and photocatalytic activity. *Materials Science Forum*, 883, pp. 23-28. [doi:10.4028/www.scientific.net/MSF.883.23]
- bdul Ghani, S. A., Hamid, M. A. A., Lah, N. A. C. & Arifin, Z. (2017). Optimization and characterization of silicon dioxide nanoparticles by sol-gel method. *Materials Today: Proceedings*, 4, 9, pp. 9221-9226.
- Biradar, A. I., Sarcalkar, P. D., Tell, S. R., Pawar, C. A., Patil, P. S. & Prasad, N. R. (2021). Photocatalytic degradation of dyes using one-step synthesized silica nanoparticles. *Materials Today Proceedings*, 43(S1): doi:[10.1016/j.matpr.2020.11.946](https://doi.org/10.1016/j.matpr.2020.11.946)
- Cui, H., Zhu, H., & Yang, X. (2011). A facile method for large-scale preparation of silicon nanoparticles from rice straw ash. *Materials Letters*, 65, 24, pp. 3704-3706, doi:10.1016/j.matlet.2011.10.014.
- Daulay, A., Andriyani., Marpongahtun & Gea, S. (2022). Synthesis Si nanoparticles from rice husk as material active electrode on secondary cell battery with X-Ray diffraction analysis. *South African Journal of Chemical Engineering*, 42, pp. 32-41, <https://doi.org/10.1016/j.sajce.2022.07.004>
- Daulay, M. R., Husin, H. & Djaja, N. A. (2022). Synthesis and characterization of silica nanoparticles from silica sand by using ball milling and heating process. *Materials Today: Proceedings*, 55, pp. 1323-1327.
- Dube, S., Soni, S. K., Sinha, M. K., Srivastava, A. & Ahluwalia, A. S. (2022). Evaluation of agricultural waste biomass for





- sustainable energy and environmental applications: A review. *Renewable and Sustainable Energy Reviews*, 154, 111904.
- Ebadi, M., Taheri-Nassaj, E., & Aghaei, A. (2009). Determination of the kinetic parameters of carbon dioxide adsorption on activated carbon particles: A multi-BET approach. *Chemical Engineering Journal*, 155, 1-2, pp. 625-631.
- Eddy, N. O., Edet, U. E., Oladele J. O., Kelle, H. I., Ogoko. E. C., Odiongenyi, A. O., Ameh, P., Ukpe, R. A., Ogbodo, R., Garg, R. & Garg, R. (2023f). Synthesis and application of novel microporous framework of nanocomposite from trona for photocatalysed degradation of methyl orange dye. *Environmental Monitoring and Assessment*. doi : 10.1007/s10661-023-12014-x,
- Eddy, N. O., Garg, R., Garg, R., Aikoye, A. & Ita, B. I. (2023h). Waste to resource recovery: mesoporous adsorbent from orange peel for the removal of trypan blue dye from aqueous solution. *Biomass Conversion and Biorefinery*, 13, pp. 13493-13511, doi: 10.1007/s13399-022-02571-5.
- Eddy, N. O., Garg, R., Garg, R., Eze, S. I., Ogoko, E. C., Kelle, H. I., Ukpe, R. A., Ogbodo, R. & Chijoke, F. (2023b). Sol-gel synthesis, computational chemistry, and applications of CaO nanoparticles for the remediation of methyl orange contaminated water. *Advances in Nano Research*, <https://doi.org/10.12989/anr.2023.15.1.000>.
- Eddy, N. O., Garg, R., Garg, R., Garg, R., Ukpe, R. A. & Abugu, H. (2024d). Adsorption and photodegradation of organic contaminants by silver nanoparticles: isotherms, kinetics, and computational analysis. *Environ Monit Assess*, 196, 65, <https://doi.org/10.1007/s10661-023-12194-6>.
- Eddy, N. O., Garg, R., Garg, R., Ukpe, R. A. & Abugu, H. (2023e). Adsorption and photodegradation of organic contaminants by silver nanoparticles: isotherms, kinetics, and computational analysis. *Environmental Monitoring and Assessment*, doi : 10.1007/s10661-023-12194-6,
- Eddy, N. O., Garg, R., Ukpe, R. A., Akpanudo, N. W., Abugu, H., Garg, R., Anjum, A. & Anand, B. (2024a). Chapter Ethical issues Chapter 10: Ethical and environmental implication associated with the application of nanoparticles. doi:: 10.4018/979-8-3693-1094-6.ch010. pp. 274-299.
- Eddy, N. O., Garg, R., Ukpe, R. A., Ameh, P. O., Gar, R., Musa, R., Kwanchi, D., Wabaidur, S. M., Afta, S., Ogbodo, R., Aikoye, A. O. & Siddiqui, M. (2024c). Application of periwinkle shell for the synthesis of calcium oxide nanoparticles and in the remediation of Pb<sup>2+</sup>-contaminated water. *Biomass Conversion and Biorefinery*, doi 10.1007/s13399-024-05285-y.
- Eddy, N. O., Jibrin, J. I., Ukpe, R. A., Odiongenyi, A. O., Kasiemobi, A. M., Oladele, J. O. & Runde, M. (2024b). Experimental and theoretical investigations of photolytic and photocatalysed degradations of crystal violet Dye (CVD) in water by oyster shells derived CaO nanoparticles (CaO-NP), *Journal of Hazardous Materials Advances*, 100413, <https://doi.org/10.1016/j.hazadv.2024.100413>.
- Eddy, N. O., Odiongenyi, A. O., Garg, R., Ukpe, R. A., Garg, R., El Nemir, A., Ngwu, C. M. & Okop, I. J. (2023c). Quantum and experimental investigation of the application of *Crassostrea gasar* (mangrove oyster) shell-based CaO nanoparticles as adsorbent and



- photocatalyst for the removal of procaine penicillin from aqueous solution. *Environmental Science and Pollution Research*, doi:10.1007/s11356-023-26868-8. .
- Eddy, N. O., Ukpe, R. A., Ameh, P., Ogbodo, R., Garg, R. & Garg, R. (2023g). Theoretical and experimental studies on photocatalytic removal of methylene blue (MetB) from aqueous solution using oyster shell synthesized CaO nanoparticles (CaONP-O). *Environmental Science and Pollution Research*, <https://doi.org/10.1007/s11356-022-22747-w>.
- Eddy, N. O., Ukpe, R. A., Garg, R., Garg, R., Odionenyi A. O., Ameh, P. & Akpet, I. N. (2023b). Enhancing water purification efficiency through adsorption and photocatalysis: models, application and challenges. *International Journal of Environmental Analytical Chemistry*, doi: 10.1080/03067319.2023.2295934.
- Eddy, N. O., Ukpe, R. A., Garg, R., Garg, R., Odionenyi, A. O., Ameh, P., Akpet, I. N. & Udo, E. S. (2023a). Review of in-depth knowledge on the application of oxides nanoparticles and nanocomposites of Al, Si and Ca as photocatalysts and antimicrobial agents in the treatment of contaminants in water. *Clean Technologies and Environmental Policy*, doi: 10.1007/s10098-023-02603-2
- Faria, P. C. C., Pereira, S. I. S. & Oréface, R. L. (2016). Silicon nanoparticles from sugarcane bagasse ash: Synthesis and characterization. *Materials Research*, 19, 2, pp. 332-338, doi:10.1590/1980-43682016000090002.
- Faria, P. C. C., Santana, R. C., de Albuquerque, T. N. & Oréface, R. L. (2022). Synthesis and characterization of silicon nanoparticles from corn cobs using a sustainable approach. *Ceramics International*, 48, 18, pp. 26250-26258. [doi:10.1016/j.ceramint.2022.05.142]
- Fernandes, F. M., Sousa, A. F., Gaspar, M., Pereira, M. F. R., & Freire, C. S. R. (2014). Silicon nanoparticles from eucalyptus bark ash: A new approach for sustainable synthesis. *Industrial Crops and Products*, 52, pp. 378-384. [doi:10.1016/j.indcrop.2013.12.021]
- Garg, R., Garg, R. & Eddy, N. O. (2024). Chapter 4: Applications of nanocomposites in water remediation: A mechanistic Overview, doi: 10.4018/979-8-3693-1094-6.ch004
- Garg, R., Garg, R., Parkash, C. & Eddy, N. O. (2023). Neutrosophic cross entropy-based discrimination of antioxidant potential and polyphenolic contents of potential and polyphenolic content of *Arisaema fortuneum*. *Neutrosophic Sets and Systems*. 61, pp. 69-88. DOI: 10.5281/zenodo.10428595.
- Garg, R., Garg, R., Eddy, N. O., Almohana, A. I., Fahad, S., Khan, M. A. & Hong, S. H. (2022). Biosynthesized silica-based zinc oxide nanocomposites for the sequestration of heavy metal ions from aqueous solutions. *Journal of King Saud University-Science* <https://doi.org/10.1016/j.jksus.2022.101996>
- Garg, R., Mittal, M., Tripathi, S., & Eddy, N. O. (2024). Core to concept: synthesis, structure, and reactivity of nanoscale zero-valent iron (NZVI) for wastewater remediation. *Environmental Science and Pollution Research*. Advance online publication. <https://doi.org/10.1007/s11356-024-33197-x>
- Hodhod, O., Khallafalla, M. S. & Osman, M. S. M. (2019). ANN models for nano silica/silica fume concrete strength prediction, *Water Science*, 33, 1, pp. 118-127. doi: [10.1080/-11104929.2019.1669005](https://doi.org/10.1080/-11104929.2019.1669005)
- Hodhod, R., Aftab, M., Abbas, N., & Qaisar, S. (2019). Preparation and characterization of silica nanoparticles from rice husk ash



- using ultrasonication. *Silicon*, 11, 5, pp. 2253-2259.
- Hussin, R., Abdullah, M. M. A. B., Muhamad, M. R., Rusop, M., & Abdullah, S. (2016). Preparation and characterization of silicon dioxide nanoparticles synthesized via a sol-gel process. *Results in Physics*, 6, pp.625-631.
- Intartaglia, B., Bagga, K., Scotto, M., Diaspro, A. and Brandi, F. (2012). Luminescent silicon nanoparticles prepared by ultra short pulsed laser ablation in liquid for imaging applications. *Optical Materials*, 2, pp. 510-518
- John, B., Namisul Gani, A. H., & Ramli, M. Z. (2014). Green synthesis of silicon nanoparticles from coconut shell using solution combustion method. *Ceramics International*, 40(12, Part B), 15277-15283. [doi:10.1016/j.ceramint.2014.07.090]
- Kao, M. J., Hsu, F. C., & Peng, D. X. (2014). Synthesis and characterization of SiO<sub>2</sub> nanoparticles and their efficacy in chemical mechanical polishing steel substrate. *Advances in Materials Science and Engineering*. <https://doi.org/10.1155/2014/691967>
- Kelle, H. I., Ogoko, E. C., Akintola O and Eddy, N. O. (2023). Quantum and experimental studies on the adsorption efficiency of oyster shell-based CaO nanoparticles (CaONPO) towards the removal of methylene blue dye (MBD) from aqueous solution. *Journal: Biomass Conversion and Biorefinery*, doi:10.1007/s13399-023-04947-7.,
- Kumar, A., Rai, D. C., & Singh, N. (2019). A facile green synthesis of silicon nanoparticles from *Leucaena leucocephala* leaves and their potential application for dye degradation. *Journal of Alloys and Compounds*, 781, 120923. [doi:10.1016/j.jallcom.2018.12.092]
- Kumar, S., Nehra, M., & Dilbaghi, N. (2019). Silicon dioxide nanoparticles: A review of preparation, properties, and applications. *Materials Science and Engineering: C*, 98, pp. 1127-1158.
- Li, B., Luo, M., & Li, J. (2020). Preparation and characterization of porous silica nanoparticles for the controlled release of poorly water-soluble drug quercetin. *Journal of Drug Delivery Science and Technology*, 56, 101521.
- Li, H., Zhang, Q., Yan, X., et al. (2020). Synthesis of Micro Porous SiO<sub>2</sub> Nanoparticles with Enhanced Adsorption Capacity for Methylene Blue Removal. *Materials Research Express*, 7, 6, 065516. <https://doi.org/10.1088/2053-1591/ab83bb>
- Li, H., Zhang, Q., Yan, X., et al. (2020). Synthesis of Micro Porous SiO<sub>2</sub> Nanoparticles with Enhanced Adsorption Capacity for Methylene Blue Removal. *Materials Research Express*, 7(6), 065516. <https://doi.org/10.1088/2053-1591/ab83bb>
- Li, X., Xiao, W., & Wang, X. (2012). Synthesis of silicon nanoparticles from peanut shells by carbothermal reduction with magnesium. *Materials Letters*, 76, 101-103. [doi:10.1016/j.matlet.2012.01.024]
- Li, X., Xiao, W., & Wang, X. (2013). Synthesis of silicon nanoparticles from cornstalk by carbothermal reduction. *Materials Research Bulletin*, 48, 10, pp. 3622-3627. [doi:10.1016/j.materresbull.2013.07.032]
- Li, X., Xiao, W., & Wang, X. (2014). Synthesis of silicon nanoparticles from cotton stalk by carbothermal reduction with magnesium. *Ceramics International*, 40, 15, pp. 22821-22825.
- Li, X., Zhu, S., & Shuai, C. (2021). Silica nanoparticles synthesized from rice straw: Morphology and mechanism. *Journal of Cleaner Production*, 281, 124461.
- Murugan, A. V., Nanjan, M. J., & Elumalai, E. K. (2020). Synthesis of silica nanoparticles and their applications in



- catalysis. *Materials Today: Proceedings*, 33, pp.1103-1108.
- Odoemelam, S. A., Oji, E. O., Eddy, N. O., Garg, R., Garg, R., Islam, S., Khan, M. A., Khan, N. A. & Zahmatkesh, S. (2023). Zinc oxide nanoparticles adsorb emerging pollutants (glyphosate pesticide) from aqueous solution. *Environmental Monitoring and Assessment*, <https://doi.org/10.1007/s10661-023-11255-0>
- Odoemelam, S. A., Oji, E. O., Eddy, N. O., Garg, R., Garg, R., Islam, S., Khan, M. A., Khan, N. A. & Zahmatkesh, S. (2023). Zinc oxide nanoparticles adsorb emerging pollutants (glyphosate pesticide) from aqueous solution. *Environmental Monitoring and Assessment*, <https://doi.org/10.1007/s10661-023-11255-0>.
- Ogoko, E. C., Eddy, N. O. & Ujam, O. T. (2023). Synthesis of copper oxide nanoparticles using Dioscorea bulbifera L. tuber aqueous extract: A mechanistic approach. *Journal of Taibah University for Science*, 17, 1, pp. 1740-1749.
- Ogoko, E. C., Kelle, H. I., Akintola, O. & Eddy, N. O. (2023). Experimental and theoretical investigation of Crassostrea gigas (gigas) shells based CaO nanoparticles as a photocatalyst for the degradation of bromocresol green dye (BCGD) in an aqueous solution. *Biomass Conversion and Biorefinery*. <https://doi.org/10.1007/s13399-023-03742-8>.
- Ogoko, E. C., Kelle, H. I., Akintola, O. & Eddy, N. O. (2023). Experimental and theoretical investigation of Crassostrea gigas (gigas) shells based CaO nanoparticles as a photocatalyst for the degradation of bromocresol green dye (BCGD) in an aqueous solution. *Biomass Conversion and Biorefinery*. <https://doi.org/10.1007/s13399-023-03742-8>.
- Oladejo, O. O., Olowokere, T. A., & Ebenso, E. E. (2021). Synthesis and characterization of silicon nanoparticles from mango peels for potential application in dye wastewater treatment. *Journal of Materials Science: Materials in Electronics*, 32, 20, pp. 17627-17640.
- Rahimzadeh, M., Farajzadeh, R., Fazli, M., & Ghamari, M. (2022). Green synthesis of silica nanoparticles using oak wood ash extract: Characterization and its application. *Materials Chemistry and Physics*, 279, 125755.
- Singh, J., Singh, S., & Singh, A. (2022). Rice husk as a biosorbent for removal of heavy metal ions from wastewater: A review. *Journal of Environmental Chemical Engineering*, 10(1), 108038.
- Singh, S., Singh, G., & Kim, K. H. (2018). Synthesis of silicon nanoparticles from orange pulp for potential applications. *Ceramics International*, 44, 13, pp. 15806-15812.
- Srivastava, S., Sinha, M. K., & Dubey, R. (2021). Synthesis of nanostructured SiO<sub>2</sub> from rice husk: A comprehensive review. *Silicon*, 13, 11, pp. 2497-2518.
- Zhang, L., Qin, Z., Zhang, H., & Liu, Z. (2021). Microporous silica nanoparticles: Synthesis, functionalization, and applications in drug delivery and adsorption. *Nanoscale Research Letters*, 16, 1, 33-40. .
- Zhang, L., Wang, Y., Zhao, Y., et al. (2021). Micro Porous Silica Nanoparticles Loaded with Isoniazid for Tuberculosis Treatment. *Journal of Nanomaterials*, 2021, 6643298. <https://doi.org/10.1155/2021/6643298>.
- Zhang, L., Wang, Y., Zhao, Y., et al. (2021). Micro Porous Silica Nanoparticles Loaded with Isoniazid for Tuberculosis Treatment. *Journal of Nanomaterials*, 2021, 6643298. <https://doi.org/10.1155/2021/6643298>.



**Compliance with Ethical Standards**

**Declaration**

**Ethical Approval**

Not Applicable

**Competing interests**

The authors declare that they have no known competing financial interests or personal relationships that could have appeared to influence the work reported in this paper.

**Funding**

The authors declared no source of funding

**Availability of data and materials**

Data would be made available on request.

**Authors contributions**

Fabian: Conceptualization, experimental and manuscript. Mfon: experimental and manuscript development

